Proc. of the 9th Intl. Conf. of Asian Society for Precision Engg. and Nanotechnology (ASPEN 2022)
15–18 November 2022, Singapore. Edited by Nai Mui Ling Sharon and A. Senthil Kumar
doi://10.3850/978-981-18-6021-8_OR-15-0111

High-speed multi-Line structured-light 3-D scanning system for accurate surface profilometry

Bo-Han Huang[1], Yuan-Fu Tsao[1], Fu-Sheng Yang[1] and Liang-Chia Chen[1,#]
1 Department of Mechanical Engineering, National Taiwan University, No. 1, Section 4, Roosevelt Rd., Taipei City, 10617, Taiwan
Corresponding Author / Email: lchen@ntu.edu.tw

KEYWORDS: Surface profilometry, laser triangulation, structured-light, 3D reconstruction, precision metrology.

A method for precision surface profilometry by applying a novel galvanometer-scanned multi-line Optomechatronics design principle is proposed. Based on the structured-light triangulation scanning principle, the proposed system was realized in a single integrated optical module while remaining excellent height measuring resolution and precision with a high-speed imaging sensor. In work, different from the traditional laser line generator, a cylindrical array lens is designed as a condenser, and a green light-emitting diode (LED) is used to generate multiple linear light beams that can be projected and manipulated by a galvanometer as a scanning structured-light projector, and avoid the uncertainty that comes from transitional laser speckle effect. The proposed method can avoid the disadvantages of the traditional laser triangulation scanning methods relying on the movement of measuring objects, which increases uncertainties introduced by positioning uncertainty incurred from conveyor belts or mechanical stages. With a precise galvanometer mirror integrated into the scanning system, the scanning uncertainty can be significantly reduced to achieve high precision 3D measurement speedily. Moreover, the developed system is designed to achieve a micron-level measuring accuracy by applying a novel sub-micron peak detection algorithm. Verified by experimental tests, the developed method is capable of measuring a highly scattered surface of metallic surfaces made by the directed energy deposition (DED) 3-D printing process, and the depth accuracy can reach better than 20 micrometers with a measuring time of less than 2 seconds.

NOMENCLATURE

(u, v): Image pixel coordinate.

Δu: The pixel-wise lateral shifting of peak points on the light stripe that is caused by height change.

(x_w, y_w, z_w): World coordinate.

1. Introduction

Recently, the demand for high precision and high-speed measuring systems has grown exponentially in metrology as the manufactured products become miniaturized. To detect and resolve the problem encountered in the manufacturing process, optical inspection systems are usually integrated into the production line to monitor the yield rate of the product for automated optical inspection (AOI).

Automatically inspecting the manufactured parts in the product line to attain efficient quality control is a paradigm in the manufacturing industry where the laser triangulation scanning method is often implemented. Laser triangulation utilizes a laser as a fixed structured light source, and the object to be inspected is placed on a scanning stage that moves at a constant speed. The object's profile can then be obtained when the object passes through the laser scan. However, the profile of measuring objects may be distorted due to the inconsistent moving speed of the stage. Also, the laser source is highly coherent, which may induce non-uniform light intensity called the speckle effect. This effect may also lead to erroneous height calculations in the algorithm.

To cope with inconsistent scanning speed in the traditional method, we proposed a 3-D optical surface profilometric system equipped with a galvanometer mirror. Using a galvanometer mirror can eliminate the uncertainty introduced by environmental disturbances. Moreover, this kind of measuring system can also be widely used in general since it has better scanning flexibility and efficiency than the traditional method. The laser light source is replaced by LED in the proposed system to tackle the speckle effect since the coherence of LED is lower. Moreover, the applied LED also has a lower cost and longer lifetime than the laser light source, making the proposed system more affordable and easier to set up for in-line operations.

2. Method

2.1 Optical System Design

As shown in Fig.1, the proposed system can be roughly divided into the structured-light projecting subsystem and imaging module[1]. LED emits light at a wide angle in the projection system, so a condenser lens is placed in front of the LED light source to collimate the light rays. Next, a cylinder lens array transforms the collimated light into a multi-line structured-light pattern, which projects three straight lines onto the measuring plane. To establish a scanning mechanism, a reversed F-θ lens projects the structured light onto a mirror at an angle that can be precisely controlled by a Galvanometer. Finally, the light is reflected to another F-θ lens and then projected onto the measuring plane to form a 40 mm x 40 mm squared scanning region as the scanning field of view (FOV).

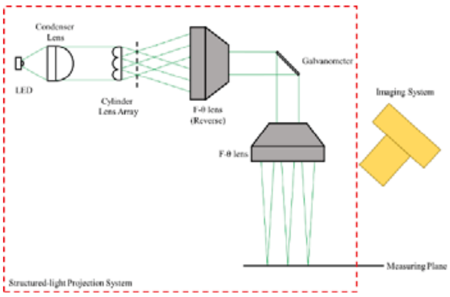

Fig. 1 Setup of the proposed structured-light triangulation scanning system.

Due to the limitation of commercial F-θ lenses, the LED light source in the system is chosen to be an LED module with peak intensity at wavelength 532 nm. Many researchers have shown different types of applications that collimate the light luminesced by an LED, Fresnel lens [2] or microlens array combined with prism array [3], and freeform lens consists of a parabolic lens and an elliptic lens [4]. Although these methods collimate the light rays well, the intensity distribution is usually non-uniform after collimation. In the proposed system, a commercial aspheric condenser lens is used to collimate the light beam, while containing a uniform distribution of the light intensity within the projection area.

The cylindrical lens array applied in the system is 1-inch x 1-inch in size, which contains three cylindrical surfaces per inch. To verify whether the system can generate linear structured-light patterns, a simulation is conducted by using Zemax OpticStudio (Shown in Fig. 2).

There is a similar way to convert a point light source into the linear structured-light pattern by using a cylindrical lens array [5], where the light is focused on one axis and diverged on the other perpendicular axis (Fig.3). However, since the power of an LED module is usually smaller than a laser light source, the proposed method can obtain a high lighting efficiency when converting collimated light into multi-line structured-light.

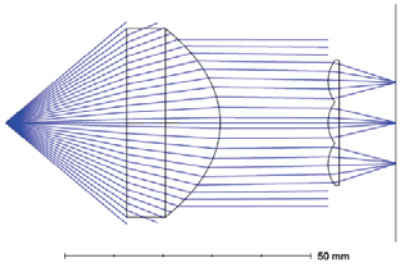

Fig. 2 Optical simulation of light rays from source to structured-light pattern using Zemax OpticStudio. The condenser lens collimates the light rays, then passes through the cylindrical lens array.

F-θ lenses have been widely used in laser scanning systems. F-θ lenses have a flat imaging plane, so each line in the structured light is equally focused on the imaging plane. Generally, suppose the wavelength of the light source is within a small range. In that case, the relationship between the distance of the projected light spot from the optical axis (Δy) and the incident angle (θ) can be expressed by the following equation[6]:

$$\Delta y = f \cdot \theta \tag{1}$$

in which f is the focal length.

This equation shows a linear relationship between Δy and θ. Thus, the structured-light scan rate is fixed if the galvanometer rotates at a constant speed.

The light trace simulation of the structured-light projection system is also conducted (Fig.3).

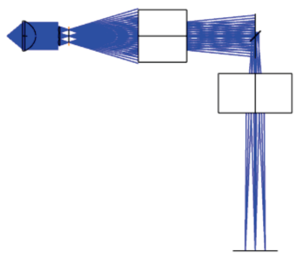

Fig. 3 Optical simulation of the structured-light projection system.

2.2 Measurement Algorithm

2.2.1 Space Mapping Function

The algorithm in the proposed system utilizes a customized space mapping function to extract height information from the structured-light peak position in 2D images. The space mapping function[7] is essentially a polynomial function where its inputs are combinations of pixel coordinates (u, v) and the pixel-wise shifted distance of the peaks of the structured-light stripes (Δu) (as shown in Fig. 4) [8]. Outputs are the real-world coordinates (x_w, y_w, z_w) corresponding to the pixel coordinates (u, v) and lateral shifted distance (Δu). The relationship between $(u, v, \Delta u)$ and (x_w, y_w, z_w) is shown as (Eq.(2)).

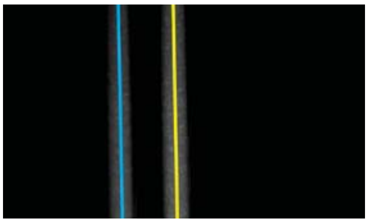

Fig. 4 Δu is defined as the lateral pixel-wise distance between blue and yellow peak points. The blue line represents peaks of structured-light stripes on the reference plane, and the yellow line represents peaks of structured-light stripes at a certain height z_w.

$$\begin{bmatrix} x_w \\ y_w \\ z_w \end{bmatrix} = \sum_{k=0}^{n} \sum_{j=0}^{n-k} \sum_{i=0}^{n-k-j} \begin{bmatrix} a_{ijk} \\ b_{ijk} \\ c_{ijk} \end{bmatrix} u^i v^j \Delta u^k \quad (2)$$

By fitting this polynomial model to real-world data and applying the least squares approximation method, the best coefficients $(a_{ijk}, b_{ijk}, c_{ijk})$ can be obtained. The residual error of the model is defined to be the Euclidean distance between real-world coordinates $(x_{w,p}, y_{w,p}, z_{w,p})$ and predicted coordinates $(\widehat{x_{w,p}}, \widehat{y_{w,p}}, \widehat{z_{w,p}})$.

$$res = \sum_{p=0}^{N} \sqrt{\left(\widehat{x_{w,p}} - x_{w,p}\right)^2 + \left(\widehat{y_{w,p}} - y_{w,p}\right)^2 + \left(\widehat{z_{w,p}} - z_{w,p}\right)^2} \quad (2)$$

The purpose of the least squares method is to minimize the residual error (res) stated above. In practice, the Levenberg-Marquardt method [9, 10] is used as the least square algorithm. In this research, n = 3 is used to design the space mapping function.

2.2.2 Building Database for Mapping Function

To ensure that the model can be used in the proposed system, the real-world data should be uniformly sampled by the system in the measurable region (Fig. 5). To do so, the measurable region is segmented into several equidistant height levels. The structured-light projecting system should be able to scan on each level.

For each height level, a chessboard is used to calibrate the imaging system, and a transformation matrix is obtained after camera calibration. Next, perform a structured-light scanning and extract the pixels in the image where the structured light has peak intensity. Using the transformation matrix, these pixels can define the value of (u, v, x_w, y_w). Compare the pixels where the structured light has a peak intensity at the reference height and the current measured height. Perform the mapping from the shifted lateral pixel-wise distance (Δu) to the current measured height (z_w). Repeat the process stated above for each height level.

These data points are composed of 6 elements $(x_w, y_w, z_w, u, v, \Delta u)$ and then stored in the database for model fitting.

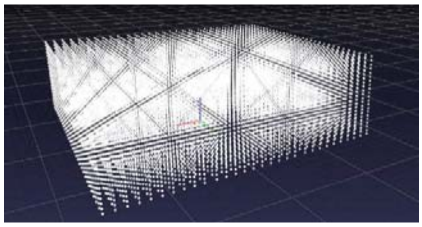

Fig. 5 Uniformly sampled points $(x_w,\ y_w,\ z_w)$ in the measuring space.

3. Measurement Results

3.1 Errors of space mapping function results

First, to confirm the precision result of space mapping functions, we compare RMS errors of dataset points between predicted results $(\widehat{x_{w,p}}, \widehat{y_{w,p}}, \widehat{z_{w,p}})$ and ground-truth data $(x_{w,p}, y_{w,p}, z_{w,p})$ in three axes. The result is shown in Table 1.

Table 1 RMS errors of mapping function in three axes.

	X-axis	Y-axis	Z-axis
RMS error (mm)	0.008	0.002	0.017

The result shows that the precision of results predicted by the mapping function can reach the micrometer level in the lateral direction and a level of less than 20 micrometers in the height direction.

3.2 Semi-sphere measurement

For sphere measurement, by measuring two semi-spheres and detecting the distance between two centers, we can verify the ability to measure different surface profiles in the measuring space. The result is compared with the result measured by a precise coordinate measuring machine (CMM) manufactured by Mitutoyo, with a 0.8 µm accuracy. We conducted 30 times for both measuring systems to evaluate the accuracy and precision performance. The photo of the semi-sphere sample is shown in Fig. 6.

The point cloud result is shown in Fig.6, and the distance result is shown in Table 2.

Results show that the proposed system has a great precision performance with a 6 µm standard deviation, and the average error compares to the result measured by CMM also shows that this system has a great ability to conduct high-accuracy profilometry.

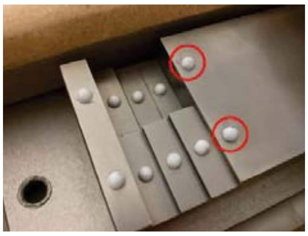

Fig. 6 Semi-sphere sample. The distance between two semi-spheres marked by red circles is detected.

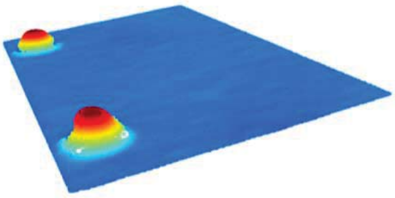

Fig.7 Point cloud result of semi-spheres sample.

Table 2 Distance measuring result of semi-sphere sample.

	Average sphere center distance (mm)	Standard deviation (mm)
CMM	24.9817	0.0004
Proposed system	24.957	0.006
Bias Error	-0.025	

3.3 Metallic parts measurement

In the research, we also measured a real part made by the directed energy deposition (DED) 3-D printing process, to show the 3-D profilometry ability of this system. The photo of the metallic sample is shown in Fig. 8.

Fig. 8. DED metallic sample.

The measured point clouds map of the test sample is shown in Fig. 9. From the result, it shows that this system can reconstruct the surface structure on the sample, showing that this system has its ability to achieve precision surface profilometry measurement even on a surface with scattering reflectivity. This indicates that the developed system outperforms the other traditional laser triangulation probes in handling a scattering surface.

4. Conclusions

This research proposes a high-speed multi-line structured-light 3D profilometry scanning system. The innovative optical design of the structured-light projection system can evenly project thin lines onto the measuring surface, thus making this scanning system have an extraordinary performance within a small amount of time. LED light source is used to reduce the speckle effect due to the coherence of laser light and also increase the lifetime of this system. Verified by experiment results, the developed system is capable of achieving a 20-μm accuracy measurement with high precision. When the light efficiency is optimized, the Galvo-scanning system can reach its maximum scanning speed of 800 lines/second. Furthermore, the developed system outperforms the traditional laser triangulation probes in handling a scattering surface.

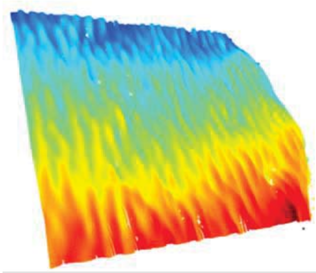

Fig. 9. Point cloud measured result of the DED metallic sample shown in Fig. 8.

References

1. G. F. Marshall and G. E. Stutz, *Handbook of optical and laser scanning*. Taylor & Francis, 2012.
2. A. McCarthy, J. Romero-Vivas, C. O'Hara, N. Rebrova, L. Lewis, and S. P. Hegarty, “LED-Based Collimating Line-Light Combining Freeform and Fresnel Optics,” *IEEE Photonics Journal*, vol. 10, no. 6, pp. 1-13, 2018.
3. E. Aslanov, L. L. Doskolovich, and M. A. Moiseev, “Thin LED collimator with free-form lens array for illumination applications,” *Applied Optics*, vol. 51, no. 30, pp. 7200-7205, 2012.
4. D. Vázquez-Moliní, M. G. Montes, A. A. Fernandez-Balbuena, and E. B. Martinez, “High-efficiency light-emitting diode collimator,” *Optical Engineering*, vol. 49, no. 12, p. 123001, 2010.
5. M. Rückwardt, A. Göpfert, G. Linß, and S. Kienast, “A structured LED linear light as an economically priced and technical alternative to a laser line generator,” in *20th IMEKO TC2 Symposium on Photonics in Measurement, Linz, Austria*, pp. 16-18, 2011.
6. J. Breckinridge, Y. Ji, Y. Wang, W. Shen, and J. Yu, "Large working area F-Theta lens," presented at the ICO20: Optical Design and Fabrication, 2006.
7. M. Chang, K. Lin, “Non-contact scanning measurement utilizing a space mapping method,” Optics and Lasers in Engineering, vol. 30, no. 6, pp. 503-512, 1998.

8. C. Steger, "An unbiased detector of curvilinear structures," *IEEE Transactions on pattern analysis and machine intelligence,* vol. 20, no. 2, pp. 113-125, 1998.
9. J. J. Moré, "The Levenberg-Marquardt algorithm: implementation and theory," in *Numerical analysis*: Springer, 1978, pp. 105-116.
10. K. Levenberg, "A method for the solution of certain non-linear problems in least squares," *Quarterly of applied mathematics,* vol. 2, no. 2, pp. 164-168, 1944.